Formation of protons from dissociative ionization of methane induced by 54 eV electrons

S. Xu,[1,2,3] X. Ma,[1,*] X. Ren,[2] A. Senftleben,[2] T. Pflüger,[2] A. Dorn,[2,†] and J. Ullrich[2]

[1]*Institute of Modern Physics, Chinese Academy of Sciences, Lanzhou 730000, China*

[2]*Max-Planck-Institut für Kernphysik, Saupfercheckweg1, D-69117 Heidelberg, Germany*

[3]*Graduate University of Chinese Academy of Sciences, Beijing 100049, China*

(Received 20 February 2011; published 12 May 2011)

The production mechanisms of protons in dissociation of methane by 54 eV electron impact is investigated using the reaction microscope. By measuring all three charged particles in the final state in triple coincidence, the energy deposited in the target is determined. It is found that the $(2a_1)^{-1}(npt_2)^1$, $(2a_1)^{-1}$, $(1t_2)^{-2}(3a_1)^1$, and $(2a_1)^{-2}(3a_1)^1$ states of the intermediate CH_4^+ make the major contributions to the formation of protons at this incident energy. The decay of each state results in a different kinetic energy distribution of protons. Possible decay mechanisms of these states are analyzed.

DOI: 10.1103/PhysRevA.83.052702 PACS number(s): 34.80.Ht

I. INTRODUCTION

Extensive studies of the ionization and dissociation of molecules have been carried out in previous studies by using various projectiles such as ions [1–3], photons [4–7], and electrons [8–10]. The main purposes of such studies are to investigate the various decay pathways and to clarify which parameters determine these decay pathways. Previous ion impact experiments [1–3] show that the amount of energy deposited into the target molecules is the key parameter that determines the decay pathways, and this energy deposition depends strongly on the projectile's properties (element, charge and velocity, etc.). In contrast to ion impact, the amount of energy absorbed by the target for electron impact is mainly influenced by the electron velocity. Additionally, unlike the photoionization process where a definite amount of energy is absorbed by the target, a broad range of energies can be deposited in the electron impact ionization processes and, thus, many dissociation pathways can be activated in a single experiment. If the energy transfer into the target is determined experimentally, electron-induced dissociative ionization of molecules is an ideal system to investigate the dependence of the decay pathways on this parameter.

Methane is the simplest alkanes molecule with high symmetry (T_d point group). Its ground-state electronic configuration is $(1a_1)^2(2a_1)^2(1t_2)^6$. The dissociation of methane can be a model system for our understanding of some basic physical and chemical processes, for example, the breakup of the C-H chemical bond. In addition, it also draws great interest in numerous application fields such as plasma physics [11] and the chemistry of planetary atmospheres [12].

In the fragmentation processes induced by electron impact, various ionic and neutral fragments can be produced through different dissociation pathways. Since the neutral H atom and the positively charged proton are the lightest fragments, they always carry substantial amounts of kinetic energy [9,10]. The kinetic energy distributions (KEDs) of the fragments in the final states reveal the dynamics of how these fragments are formed and determine the energy deposition pathways in the corresponding media. In addition, as a bare nucleus, the proton does not have an excited electronic state and is much easier to be detected compared with the neutral H atom. These characteristics make the proton a sensitive probe to investigate the dissociation mechanisms of methane.

However, few experiments have measured the KEDs of protons formed from the dissociation of the methane molecules. Locht *et al.* [13,14] measured proton production as a function of appearance energies in electron impact ionization of methane and analyzed the possible decay mechanisms. However, it was difficult to give any decisive conclusions regarding the intermediate states where the protons were produced. Latimer *et al.* measured the KEDs of proton fragments in their study of the dissociation of methane induced by synchrotron radiation for photon energies from 21.6 to 56.6 eV [6]. Three groups of protons were observed with kinetic energies either below 1.2 eV, around 2.2 eV, or around 3.7 eV. The protons from the three groups were attributed to the decays from the superexcited $(2a_1)^{-1}(npt_2)^1$ $(n = 3, 4)$ states, the ionic states $(2a_1)^{-1}$ and $(1t_2)^{-2}(3a_1)^1$, and the doubly ionized states, respectively. However, the kinetic energy of 3.7 eV for protons emitted after double-ionization states turns out to be much smaller than the result in Ref. [15]. Gluch *et al.* measured the KED of protons from the dissociation of methane in electron impact reactions [9]; they found the first two groups in the proton KED as Latimer *et al.* observed. Different from these authors, they discovered an energetic group with a kinetic energy of around 6 eV instead of 3.7 eV and the authors attributed the origin of these protons to the doubly charged precursor.

The rich structures of the KEDs observed in the two measurements [6,9] indicate that several decay mechanisms may be active. However, only the KEDs of protons were measured in these experiments, and this information is not sufficient for a deeper understanding of the dissociation mechanisms. For the electron-induced dissociative ionization process, if there is an experimental approach that records the energies of all charged particles in the final state, one can deduce the energy deposited into the target and obtain the kinetic energy of the fragmented ions at the same time. Such an experiment offers more detailed information to clarify the origin of different groups of protons mentioned above and to further investigate the mechanisms of the different dissociation

*x.ma@impcas.ac.cn

†dornalex@mpi-hd.mpg.de

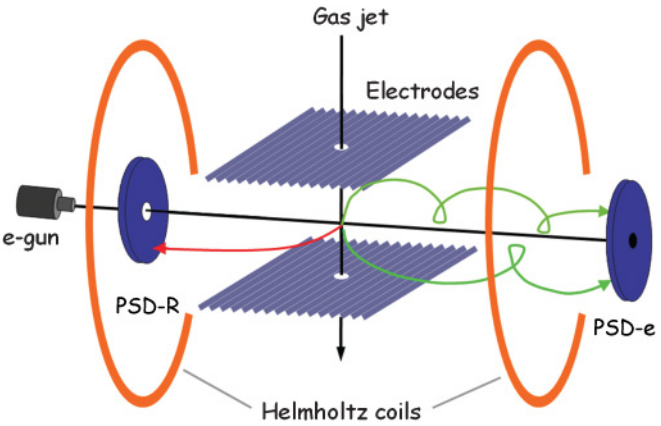

FIG. 1. (Color online) Schematic view of the reaction microscope.

channels. In the present paper, we present such an experiment performed with the advanced reaction microscope technique [16,17].

II. EXPERIMENT

The experiment was carried out with a reaction microscope specially designed for $(e, 2e)$ studies [17–19]. As shown in Fig. 1, a pulsed electron beam (with energy of 54 eV, pulse length around 1.5 ns, and repetition rate 170 kHz) crosses with the methane target produced by a two-stage supersonic gas jet. The charged fragments in the final state are extracted and directed to the two individual time- and position-sensitive detectors (PSD-R and PSD-e) by uniform electric and magnetic fields. With this experimental technique, slow protons with energy up to 1 eV are collected over the 4π solid angle. As the kinetic energy of the proton increases further, the collection efficiency gradually decreases. The collection efficiency for electrons with energies lower than 15 eV is around 80%. Owing to the high collection efficiency of the charged particles, triple coincidence measurements between two electrons and one charged fragment are performed. All the data are stored on a computer in event-by-event mode.

During offline data analysis, the initial momentum vectors of each charged particle were reconstructed according to the recorded time and position information, and thus the kinetic energies of these particles were obtained. The energy resolution is estimated to be 15% and 5% for electrons and protons, respectively.

III. RESULTS AND DISCUSSION

In order to facilitate the following discussion of the results, we first summarize in Table I the various ionized and excited states of methane observed in previous experiments. The single ionization potentials for the $(1t_2)^{-1}$ and $(2a_1)^{-1}$ states of CH_4^+ are 14.0 eV and 22.3 eV, respectively [4,12]. The $(2a_1)^{-1}(3pt_2)^1$ and $(2a_1)^{-1}(4pt_2)^1$ states are two superexcited states of CH_4 with excitation energies of 20.3 and 22.1 eV, respectively [20,21]. Since the excitation energies of the two states are higher than the ionization potential of the $(1t_2)^{-1}$ state, the CH_4 molecules in these states are unstable and can decay through the autoionization process. In addition, in previous studies of photon- or electron-induced dissociation of methane [20,22], the authors observed single ionization with simultaneous excitation of another electron (ionization-excitation). In the present experiment, the energy of the incident electron is 54 eV; thus, all the above-mentioned states are accessible.

TABLE I. Selected electronic states of methane and its positive ion observed from previous studies. Energies and electronic configurations are denoted relative to the neutral ground state. The creating processes are excitation (EX), single ionization (SI) and ionization-exciation (IE).

Energy (eV)	Electronic configuration	Creating process	References
14.0	$(1t_2)^{-1}$	SI	[4,12]
20.3	$(2a_1)^{-1}\,(3pt_2)^1$	EX	[20,21]
22.1	$(2a_1)^{-1}\,(4pt_2)^1$	EX	[20,21]
22.3	$(2a_1)^{-1}$	SI	[4,12]
25.0	$(1t_2)^{-2}\,(2t_2)^1$	IE	[22]
29.5	$(1t_2)^{-2}\,(3a_1)^1$	IE	[20,22]
34.7	$(2a_1)^{-1}\,(1t_2)^{-1}\,(2t_2)^1$	IE	[20,22]
38.6	$(2a_1)^{-2}\,(3a_1)^1$	IE	[20]

We define the energy deposition $\varepsilon_{\rm dep}$ for the electron-induced dissociation process as the energy difference between the incident electron ε_i and the two outgoing electrons ε_1 and ε_2, (i.e., $\varepsilon_{\rm dep} = \varepsilon_i - \varepsilon_1 - \varepsilon_2$). For single ionization and ionization-excitation, this value reveals the electronic states of the intermediate CH_4^+ ion before dissociation. The proton yields are shown in Fig. 2 on a relative scale as a function of the energy deposition. It can be seen from the figure that the energy deposition has a broad range and the distribution has obvious structures. These structures should result from the corresponding electronic states from which the protons are produced. A multipeak Gaussian fitting procedure was employed to separate the individual peaks from the broad distribution. The fitted results are shown by the dashed (green) lines. Four peaks centered at 18.1, 22.5, 30.0, and 39.0 eV are extracted as indicated by the vertical arrows. Comparing

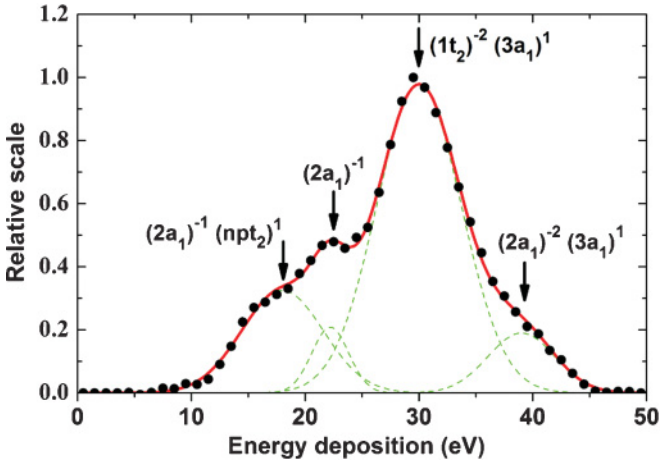

FIG. 2. (Color online) Proton yields as a function of the energy deposition. The solid circles are the experimental result. The dashed (green) lines are the fitted Gaussian peaks corresponding to different electronic states (indicated by arrows) and the solid (red) line is the sum of the fits.

the peak positions with the data of the electronic states listed in Table I, it is straightforward to identify that the last three peaks are mainly attributed to the $(2a_1)^{-1}$, $(1t_2)^{-2}(3a_1)^1$, and $(2a_1)^{-2}(3a_1)^1$ states, respectively. The first peak centered at 18.1 eV is attributed to the superexcited states, $(2a_1)^{-1}(3pt_2)^1$ and $(2a_1)^{-1}(4pt_2)^1$. Its peak energy of 18.1 eV is lower than the excitation energies of the superexcited states listed in Table I, because the energy of the autoionized electron is subtracted in the energy deposition calculation defined here. We conclude from the results of Fig. 2 that the states $(2a_1)^{-1}(npt_2)^1$, $(2a_1)^{-1}$, $(1t_2)^{-2}(3a_1)^1$, and $(2a_1)^{-2}(3a_1)^1$ contribute significantly in the formation of protons at the present incident energy.

To further investigate the correlation between the KEDs of the protons and the different electronic states shown in Fig. 2, we present the proton yields in two-dimensional correlation plots as a function of the proton kinetic energy (horizontal axis) and the energy deposition (vertical axis) in Fig. 3. Because of the decreased acceptance and the small cross sections for high-kinetic-energy protons [6,9], the number of counts in the higher-energy range is much lower than in the low-energy range. The structure in the high-energy range may be submerged in a single plot; thus, the proton yields are displayed in two separate plots [Figs. 3(a) and 3(b)] with the proton kinetic energy ranges of 0–3.5 eV and 2–7 eV, respectively. It is clear from Fig. 3(b) that there are rich structures in the high-energy range.

The intermediate electronic states producing protons are assigned as indicated in Fig. 3 according to the energy deposition. A clear image of the KEDs of protons related to different intermediate states can be seen. The protons from the autoionizing states of $(2a_1)^{-1}(npt_2)^1$ $(n = 3, 4)$ peak in an area with kinetic energies lower than 0.3 eV but extend to almost 1 eV. The protons from the $(1t_2)^{-2}(3a_1)^1$ state have a quite broad KED which ranges from 0 up to about 7.0 eV. There are two islands in the plots. One centered at around 2.3 eV is formed from the dissociation of the $(2a_1)^{-1}$ state

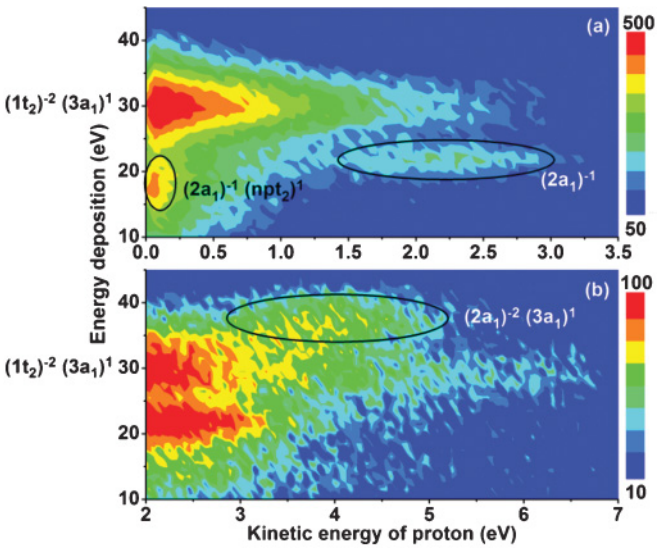

FIG. 3. (Color online) Two-dimensional plots for the proton yields as a function of the kinetic energy of the proton (horizontal axis) and the electron energy deposition (vertical axis). The ranges of the proton kinetic energy are (a) 0–3.5 eV and (b) 2.0–7.0 eV.

[Fig. 3(a)]. The other one, centered at about 3.8 eV, is formed from the $(2a_1)^{-2}(3a_1)^1$ state; its KED overlaps a little with the distribution of protons from the nearby $(1t_2)^{-2}(3a_1)^1$ state because of the close energy spacing and the energy resolution of the setup [Fig. 3(b)]. Obviously, the KEDs of the emitted protons strongly depend on the intermediate state.

Latimer *et al.* [6] found the appearance of low-energy protons at incident photon energies below the $(2a_1)^{-1}$ threshold and attributed it to dissociation of the superexcited states $(2a_1)^{-1}(npt_2)^1$ $(n = 3, 4)$. In electron impact experiments Locht *et al.* [13] observed two low-energy proton peaks at the appearance energies of 21.3 and 22.17 eV, respectively; both were interpreted as being formed through the dissociative autoionization mechanism. It is clear from the two-dimensional plots in Fig. 3 that the states $(2a_1)^{-1}(npt_2)^1$ $(n = 3, 4)$ only contribute a small part to the low-energy proton yields (<1 eV), whereas the $(1t_2)^{-2}(3a_1)^1$ state has a much higher yield of low-energy protons, which explains the rapid increase of proton production with increasing photon energy [6].

In another photoionization experiment by Furuya *et al.* [23], the authors suggested that the molecules in the $(2a_1)^{-1}(npt_2)^1$ states may decay through two pathways leading to ionic fragments: (1) autoionization takes place in the first step, and then the ionized CH_4^+ dissociates into different fragments, or (2) neutral dissociation takes place first and the autoionization of one neutral radical follows. The open question is through which pathway will the states preferentially decay? From the shape of the CH_3^+ peak observed in the time-of-flight (TOF) spectrum, the authors of Refs. [5] and [23] concluded that the $(2a_1)^{-1}(npt_2)^1$ state decays dominantly through the second pathway. In the present study, we directly observed the protons produced from the $(2a_1)^{-1}(npt_2)^1$ states in agreement with the experiments of Refs. [6] and [9], which also showed direct proton production from the same states. Since the H atom has no autoionizing state, the observation of protons is direct evidence that the first pathway also contributes to the decay of the $(2a_1)^{-1}(npt_2)^1$ states.

We illustrate our interpretation of the autoionization process leading to the production of protons in the sketched potential curves diagram of Fig. 4. We chose to represent the system in C_3v symmetry that is maintained when one proton in the methane molecule is a different distance from the carbon nucleus than the other three protons. Because energetic H atoms have been observed [20] as neutral dissociation products of the $(2a_1)^{-1}(npt_2)^1$ states, we can safely assume that their potential energy curves are at least partially repulsive along the R_{H-CH3} coordinate. Thus, excitation triggers a movement of one proton away from the remaining CH_3 core, thereby gaining kinetic energy A. As long as it is energetically allowed, autoionization to the CH_4^+ ionic states can occur, releasing an electron with energy ε_2, given by the current difference of the potential curves. In Fig. 4, an ionic state with a local minimum beneath the first $CH_3 + H^+$ dissociation limit but above the first $CH_3^+ + H$ and $CH_2^+ + H_2$ limits is imagined. A suitable minimum energy for such a state in C_3v symmetry has been reported but no corresponding energy curves or correlation diagram were given [24]. However, let us assume that after autoionization the ion is bound by the energy D. On the other side, the divergent motion of the two cores along the coordinate will continue. It can lead to dissociation with a

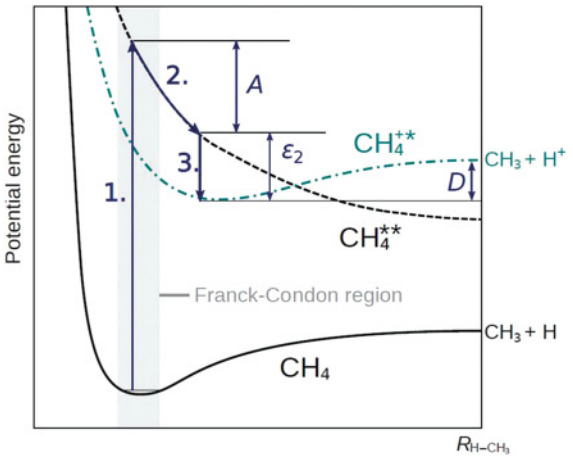

FIG. 4. (Color online) Proposed diagram of selected potential energy curves for the methane system in C_3v symmetry. CH_4, ground state of the neutral molecule; CH_4^{**}, superexcited state; CH_4^{+*}, excited ionic state with minimum below $CH_3 + H^+$ dissociation limit.

protonic fragment if A is larger than D. In the other case, CH_4^+ will be in a bound vibrational level, which in turn will fragment to the lower-lying $CH_3^+ + H$ or $CH_2^+ + H_2$ limits. For direct dissociation, the fragments will have the kinetic energy $A - D$ with the proton taking the major part of it. As A increases with the lifetime of the superexcited state, it is obvious that the maximum in the proton KED is at zero energy, as observed, for example, in a similar autoionization process in H_2 [25,26].

The island centered at 2.3 eV is dominantly dissociated from the $(2a_1)^{-1}$ state, which has a clear separation from the distribution from the $(1t_2)^{-2}(3a_1)^1$ state as shown in Fig. 3(a). In electron impact studies, Gluch *et al.* [9] observed a group of protons with kinetic energy around 2.35 eV. Latimer *et al.* [6] also observed a peak in their proton KED around 2.2 eV and pointed out that the $(2a_1)^{-1}$ and $(1t_2)^{-2}(3a_1)$ states contribute to the peak. From the present results we conclude that only the $(2a_1)^{-1}$ state contributes to the peak structure around 2.2 eV, and the $(1t_2)^{-2}(3a_1)^1$ state gives a continuous background to the peak. The separation of the two contributions makes it possible to analyze the decay mechanisms of the $(2a_1)^{-1}$ state.

In C_3v symmetry, the $(2a_1)^{-1}$ state of CH_4^+ is correlated with the first $H^+ + CH_3$ dissociation limit [27], which is located 18.1 eV above the methane ground state. Thus, there is an excess energy of at least 4.2 eV compared to the vertical ionization energy of the $(2a_1)^{-1}$ state that has to be taken away by the fragments. Owing to its smaller mass, the proton will receive $\frac{15}{16}$ of the totally released translational energy (i.e., at least 3.9 eV if all energy is transformed into kinetic energy). Since this is significantly larger than our measured KED between 1.5 and 3 eV, the CH_3 fragment has to be vibrationally and/or rotationally excited. Because it can store up to 4.7 eV of internal energy [12], this is energetically possible. On the other hand, a three-body breakup of the $(2a_1)^{-1}$ state into $H^+ + H + CH_2$ is not supported by these findings. The spread of the island along the horizontal axis may indicate that CH_3 radicals are populated in several vibrational levels or that an extended energy range can be accessed in the $(2a_1)^{-1}$ state through vertical transitions from the methane ground state.

In the broad energy deposition region centered around 30 eV, a variety of intermediate states can contribute. Apart from the central $(1t_2)^{-2}(3a_1)^1$ state, the ionic levels $(1t_2)^{-2}(2t_2)^1$ and $(2a_1)^{-1}(1t_2)^{-1}(2t_2)^1$ can contribute as well as many doubly excited and autoionizing neutral states converging toward the former [20]. The protons' KED distribution in this range is very broad, reaching from 0 up to almost 7 eV. It could therefore be possible that not only different states but also different dissociation mechanisms take part. Several dissociation limits producing protons can be reached: the already-mentioned first $H^+ + CH_3$ channel at 18.1 eV, the creation of electronically excited CH_3 above 23.9 eV, and three-body breakups $H^+ + H_2 + CH$ ($H^+ + H + CH_2$) at 22.7 (22.9) eV, respectively [12,23].

One possible pathway for the formation of low-energy protons is the cascade decay [23]: the excited CH_4^+ dissociates into H and excited CH_3^+ in the first step, and then a proton is emitted from the CH_3^+; that is,

$$CH_4^{*+} \rightarrow CH_3^{*+} + H,$$
$$CH_3^{*+} \rightarrow H^+ + \cdots .$$

During this process the neutral H atom may take a vast amount of the excess energy in the first step, leaving the CH_3^+ in lowly excited dissociative states, thus resulting in a small kinetic energy of the emitted proton in the second step.

According to the "ion core model" [28], the two cores in the $(1t_2)^{-2}(2t_2)^1$, $(1t_2)^{-2}(3a_1)^1$, and $(2a_1)^{-1}(1t_2)^{-1}(2t_2)^1$ states experience a strong Coulomb repulsion, which is similar to the Coulomb explosion of doubly charged molecular ions. The two fragments gain a great quantity of momentum in the repulsive explosion. So the light fragment will have much higher kinetic energies. During the explosion process the excited electron will finally stay at one of the fragments, which in turn becomes neutral. This may be a source of the observed high-energy protons. A similar process might lead to the island of protons emitted with a central kinetic energy of 3.8 eV and assigned to the $(2a_1)^{-2}(3a_1)^1$ state.

IV. SUMMARY

The production of protons from dissociation of methane by 54 eV electron impact has been explored in detail using a reaction microscope. Through the triple coincidence measurements of the two electrons and one positively charged fragment in the final state, energy deposition in the target is determined, and thus the intermediate states before dissociation can be assigned and conclusions concerning the fragmentation mechanisms can be drawn. It is found that the $(2a_1)^{-1}(npt_2)^1$, $(2a_1)^{-1}$, $(1t_2)^{-2}(3a_1)^1$, and $(2a_1)^{-2}(3a_1)^1$ states of the intermediate CH_4^+ make major contributions to the formation of the protons at this incident energy range. The KEDs of the emitted protons show strong dependence on the intermediate states, which indicates that they decay through different mechanisms. The superexcited states $(2a_1)^{-1}(npt_2)$ ($n = 3, 4$) mainly contribute to protons with kinetic energies lower than 0.3 eV. The decay of the $(1t_2)^{-2}(3a_1)^1$ state and neighboring levels results in a broad kinetic energy distribution of protons ranging from 0 to 7 eV, which indicates that the CH_4^+ ions in this state may dissociate in several pathways. The protons from the $(2a_1)^{-1}$

state form an island in the proton kinetic energy−energy deposition correlation plots and its center position and breadth indicates that the final dissociative fragments are H^+ and CH_3, and the CH_3 radicals are mainly populated in vibrationally excited states. Since the intermediate state is determined by the energy deposition during the collision, energy deposition is an effective parameter to control the properties of the final state fragments. The present experiment demonstrates the power of the reaction microscope for the investigation of the dissociative ionization process. This method could be applied to investigate the dissociation process of other molecules in the future.

ACKNOWLEDGMENTS

This work is partly supported by the National Natural Science Foundation of China under Grants No. 10979007 and No. 10674140. S.X. is grateful for support from the CAS-MPS program.

[1] H. O. Folkerts, R. Hoekstra, and R. Morgenstern, Phys. Rev. Lett. **77**, 3339 (1996).
[2] T. Mizuno, T. Yamada, H. Tsuchida, Y. Nakai, and A. Itoh, Phys. Rev. A **82**, 054702 (2010).
[3] N. Neumann *et al.*, Phys. Rev. Lett. **104**, 103201 (2010).
[4] C. R. Brundle, M. B. Robin, and H. Basch, J. Chem. Phys. **53**, 2196 (1970).
[5] O. Dutuit, M. Aït-Kaci, J. Lemaire, and M. Richard-Viard, Phys. Scr. T **31**, 223 (1990).
[6] C. J. Latimer, R. A. Mackie, A. M. Sands, N. Kouchi, and K. F. Dunn, J. Phys. B **32**, 2667 (1999).
[7] B. L. G. Bakker, D. H. Parker, and W. J. van der Zande, Phys. Rev. Lett. **86**, 3272 (2001).
[8] K. Motohashi, H. Soshi, M. Ukai, and S. Tsurubuchi, Chem. Phys. **213**, 369 (1996).
[9] K. Gluch, P. Scheier, W. Schustereder, T. Tepnual, L. Feketeova, C. Mair, S. Matt-Leubner, A. Stamatovic, and T. D. Märk, Int. J. Mass Spectrom. **228**, 307 (2003).
[10] N. Endstrasser, F. Zappa, A. Mauracher, A. Bacher, S. Feil, D. K. Bohme, P. Scheier, M. Probst, and T. D. Märk, Int. J. Mass Spectrom. **280**, 65 (2009).
[11] R. K. Janev, *Atomic and Molecular Processes in Fusion Edge Plasmas* (Plenum, New York, 1995).
[12] X. Liu and D. E. Shemansky, J. Geophys. Res. **111**, A04303 (2006).
[13] R. Locht, J. L. Olivier, and J. Momigny, Chem. Phys. **43**, 425 (1979).
[14] R. Locht, and J. Momigny, Chem. Phys. **49**, 173 (1979).
[15] P. G. Fournier, J. Fournier, F. Salama, P. J. Richardson, and J. H. D. Eland, J. Chem. Phys. **83**, 241 (1985).
[16] J. Ullrich, R. Moshammer, A. Dorn, R. Dörner, L. P. H. Schmidt, and H. Schmidt-Böcking, Rep. Prog. Phys. **66**, 1463 (2003).
[17] A. Dorn, M. Dürr, B. Najjari, N. Haag, C. Dimopoulou, D. Nandi, and J. Ullrich, J. Electron Spectrosc. **161**, 2 (2007).
[18] M. Dürr, C. Dimopoulou, B. Najjari, A. Dorn, and J. Ullrich, Phys. Rev. Lett. **96**, 243202 (2006).
[19] A. Senftleben, O. Al-Hagan, T. Pflüger, X. Ren, D. Madison, A. Dorn, and J. Ullrich, J. Chem. Phys. **133**, 044302 (2010).
[20] H. Fukuzawa, T. Odagiri, T. Nakazato, M. Murata, H. Miyagi, and N. Kouchi, J. Phys. B **38**, 565 (2005).
[21] K. Yachi, T. Odagiri, L. Ishikawa, T. Nakazato, T. Tsuchida, N. Ohno, M. Kitajima, and N. Kouchi, J. Phys. B: At. Mol. Opt. Phys. **43**, 155208 (2010).
[22] M. Kato, K. Kameta, T. Odagiri, N. Kouchi, and Y. Hatano, J. Phys. B **35**, 4383 (2002).
[23] K. Furuya, K. Kimura, Y. Sakai, T. Takayanagi, and N. Yonekura, J. Chem. Phys. **101**, 2720 (1994).
[24] R. F. Frey and E. R. Davidson, J. Chem. Phys. **88**, 1775 (1987).
[25] G. Laurent *et al.*, Phys. Rev. Lett. **96**, 173201 (2006).
[26] A. Senftleben, T. Pflüger, X. Ren, O. Al-Hagan, B. Najjari, D. Madison, A. Dorn, and J. Ullrich, J. Phys. B **43**, 081002 (2010).
[27] E. F. Van Dishoeck and W. J. Van Der Hart, Chem. Phys. **50**, 45 (1980).
[28] T. A. Field and J. H. D. Eland, J. Electron Spectrosc. **73**, 209 (1995).